Model Valence-Bond Studies of Aspects of Electron Conduction along a Linear Chain of Lithium Atoms

Richard D. Harcourt* and Michelle L. Styles

School of Chemistry, The University of Melbourne, Victoria 3010, Australia

Received: August 5, 2002; In Final Form: February 26, 2003

Two valence bond mechanisms for electron conduction along a linear chain of six or eight lithium atoms are studied using an ab initio valence bond approach. The initial step is of the type $(-)(Li_ALi_B)(Li_CLi_D)(Li_ELi_F)...(+) \rightarrow (-)(Li_ALi_B)^+(Li_CLi_D)^-(Li_ELi_F)...(+)$, in which the transferred electron occupies either the $2p\sigma_C$ atomic orbital (Pauling mechanism) or the antibonding σ^*_{CD} molecular orbital. An external potential is modeled by use of negative and positive charges located to the left and to the right of the chain of atoms. It is calculated that $(-)(LiLi)^+(LiLi)^-(LiLi)...(+) \rightarrow (-)(LiLi)(LiLi)^+(LiLi)^-...(+)$, which involves electron and positive hole transfer, as well as $(-)(LiLi)^+(LiLi)^-(LiLi)...(+) \rightarrow (-)(LiLi)^+(LiLi)(LiLi)^-...(+)$, with electron transfer only, contribute to the second electron transfer process. Resonance between the valence bond structures associated with the second step helps lower the energy of the second step of either mechanism. The antibonding molecular orbital mechanism is calculated to involve a marginally lower energy than the Pauling mechanism. The resonance stabilization that occurs in the second step is concomitant with greater positive hole delocalization than the first step. This phenomenon is illustrated for a linear polyene by use of Hückel molecular orbital theory and the free electron model for electrons in a 1-dimensional box. For both eight-atom mechanisms, the propensity for electron transfer to occur between cathode and anode increases as the size of the external potential increases.

Introduction

Electron conduction in metals is usually described and studied quantitatively using the delocalized molecular orbital (MO) band theory. Several qualitative valence bond (VB) mechanisms for electron conduction in alkali metals have been proposed,[1−10] but except for a provisional study reported in ref 10, no quantitative VB studies of the process have been published. A number of ab initio VB studies of the electronic structures of lithium clusters have been published,[9,11−18] and in ref 9, Lester and co-workers also give attention to conduction mechanisms in a qualitative manner. In this paper, we study aspects of two VB mechanisms for electron conduction along a linear chain of six and eight lithium atoms, arranged as $Li_ALi_BLi_CLi_DLi_ELi_F$ and $Li_ALi_BLi_CLi_DLi_ELi_FLi_GLi_H$, respectively. The purpose is to examine these mechanisms in both the absence and presence of model external potentials. Because at the most only eight atoms are included in the calculations, and the nature of the model potential, we stress that some of the conclusions obtained from our study could be model dependent. However, the study is able to provide useful insights into the nature of the primary canonical Lewis structures that contribute to two mechanisms of electron conduction, and indicate how the second and subsequent electron-transfer steps involve positive hole transfer away from the cathode as well as electron transfer toward the anode.

The approach adopted for each mechanism is equivalent to a one-dimensional approximation to Pauling's two-dimensional representation of the resonating VB mechanism,[1−6] with only those VB structures believed to participate directly in the conduction mechanism utilized in the treatment. Use of at least six atoms enables some comparisons to be made between the first and second electron-transfer steps.

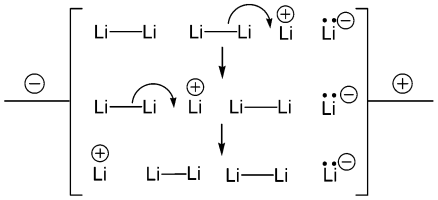

Figure 1. VB representation of the hole conduction mechanism along a linear chain of six lithium atoms.

Electron Conduction Mechanisms

We restrict our attention to mechanisms for which the initial step involves the one-electron-transfer process $(-)(Li_ALi_B)(Li_CLi_D)(Li_ELi_F)...(+) \rightarrow (-)(Li_ALi_B)^+(Li_CLi_D)^-(Li_ELi_F)...(+)$ for which the $(-)$ and $(+)$ represent the cathode and the anode. The transferred electron can then occupy either the $2p\sigma_C$ atomic orbital (AO) on Li_C (the Pauling mechanism) or the antibonding σ^*_{CD} MO.

It is to be noted that positive hole transfer, from anode to cathode, always balances the negative electron transfer, from cathode to anode. One VB formulation of this type of positive hole transfer is displayed in Figure 1. The VB structures associated with each electron-transfer step and concomitant hole transfer step participate in resonance. Electron transfer involves the formation of electron-rich bonding units, either as Li_3^- for

* Corresponding author. Fax: +613 9347 5180. E-mail address: rdharc@myriad.its.unimelb.edu.au.

10.1021/jp0266897 CCC: $25.00
Published on Web 04/12/2003

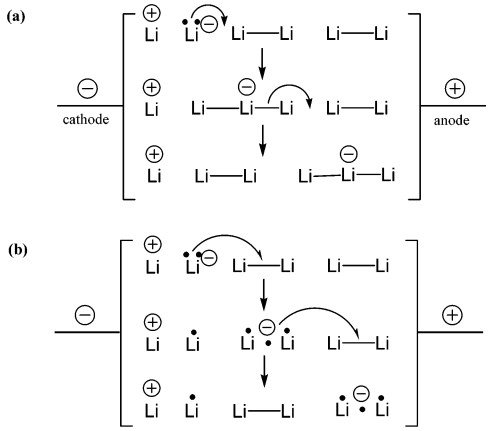

Figure 2. VB representations of (a) Pauling and (b) antibonding MO electron conduction mechanisms along a linear chain of six lithium atoms.

the Pauling mechanism (Figure 2a) or as Li_2^- for the antibonding MO mechanism (Figure 2b). In contrast, positive hole transfer involves the development of electron-deficient bonding units of the Li_3^+ type. In this paper, we restrict our attention to the electron-transfer mechanisms.

(a) Pauling Mechanism. Pauling has introduced a "metallic" orbital[1−5] in order to provide a VB representation for electron conduction in alkali metals. For lithium, this orbital is the 2pσ AO, and use of it enables "bicovalent" VB structures such as $Li^{(+)}Li-Li^{(-)}$-Li to be implicated in a "resonating VB" conduction mechanism. The results of VB calculations[14] show that bicovalent structures help to provide an appreciable contribution to the cohesive energy for the metallic solid. For a linear arrangement of six atoms, use of the bicovalent structures implies that electron conduction proceeds according to that displayed in Figure 2a,[3−5] when an electrical potential is applied.

(b) Antibonding MO Mechanism. The antibonding MO mechanism[7−10] involves the delocalization of an $Li_B^{(-)}$ electron into a vacant antibonding σ^*_{CD} MO of Li_C-Li_D, to form the (Pauling) three-electron bond configuration $(\sigma_{CD})^2(\sigma^*_{CD})^1 \propto (2s_C)^1(2s_C + k2s_D)^1(2s_D)^1$ when initially we assume that $\sigma_{CD} = 2s_C + k2s_D$ and $\sigma^*_{CD} = k^*2s_C - 2s_D$. The k is a polarity parameter, with $k^* = (k + \langle 2s_C|2s_D\rangle)/(1 + k\langle 2s_C|2s_D\rangle)$ in order that σ_{CD} and σ^*_{CD} be orthogonal. The antibonding σ^*_{CD} electron is then transferred into the antibonding σ^*_{EF} MO to create a new three-electron bond. The mechanism is displayed in Figure 2b.

(c) Modifications to Pauling and Antibonding MO Mechanisms. For both mechanisms of Figure 2, the initial conduction step involves the transfer of an electron from the ionic $Li_A^+Li_B^-$ structure into a vacant orbital. A lower energy formulation permits the ionic $Li_A^-Li_B^+$ structure to participate in resonance with the $Li_A^+Li_B^-$ structure. When this occurs, and an electron is transferred from either of the Li^- anions, the one-electron bond structure, $(Li_A{\cdot}Li_B)^+$, is obtained. This structure also arises when an electron is removed from the (Li_A-Li_B) electron-pair bond, using either a MO or a Heitler−London formulation of the wave function for this bond. The VB representations for the two mechanisms then become those of Figure 3.

In ref 10, an alternative formulation of the second electron transfer permits positive hole transfer as well as electron transfer to occur. The resulting VB representations for the mechanisms are displayed in Figure 4. The mechanisms of Figures 3 and 4 for the second step will be labeled as "electron transfer" (e_2) and "electron + hole transfer" (e_2 + h) mechanisms, respectively. The initial electron-transfer step will be designated as the (e_1) step.

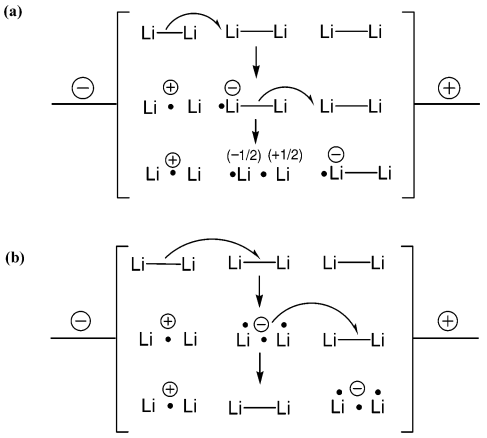

Figure 3. Modified VB representations of (a) Pauling and (b) antibonding MO electron conduction mechanisms along a linear chain of six lithium atoms, with no positive hole transfer.

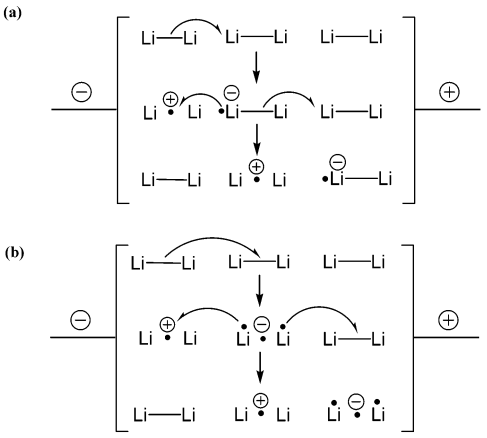

Figure 4. Modified VB representations of (a) Pauling and (b) antibonding MO electron conduction mechanisms along a linear chain of six lithium atoms, with positive hole transfer.

When Heitler−London type AO-wave functions, for example $|...2s_C^{\alpha}2s_D^{\beta}| + |...2s_D^{\alpha}2s_C^{\beta}|$, are used to represent the electron-pair bonds, each of

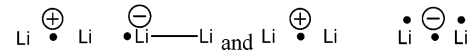

is equivalent to resonance between four (canonical) Lewis structures **1**−**4** and **5**−**8**, respectively. These structures are displayed in Figure 5.

The $Li^{(-)}$ in the Pauling mechanism involves a $(2s)^1(2p\sigma)^1$ configuration in which the 2pσ AO is used as a hybridization function, i.e., to help form an additional electron-pair bond. For the antibonding mechanism, 2pσ-orbital participation on the same atom can also be included as a polarization function, i.e., to help strengthen an existing bond. The p-orbital participation is obtained by using the $(\sigma)^2(\sigma^*)^1 = (h)^1(h + k2s')^1(2s')^1$ configuration for a Li_2^- three-electron bond structure, in which $h = 2s + \lambda 2p\sigma$. For $\lambda > 0$, resonance between the Lewis structures **5**−**8** of Figure 5 is equivalent to resonance between ten Lewis structures that involve one of the $(2s)^1$, $(2p\sigma)^1$, $(2s)^2$, $(2s)^1(2p\sigma)^1$, and $(2p\sigma)^2$ configurations for the atom or anion on which the hybrid AO is located. The $(2s)^1$ and $(2p\sigma)^1$ configurations refer to each of the structures of type **6** and **8**, and the $(2s)^2$, $(2s)^1(2p\sigma)^1$, and $(2p\sigma)^2$ configurations refer to each of the structures of types **5** and **7**. Thus, when the 2pσ AO is

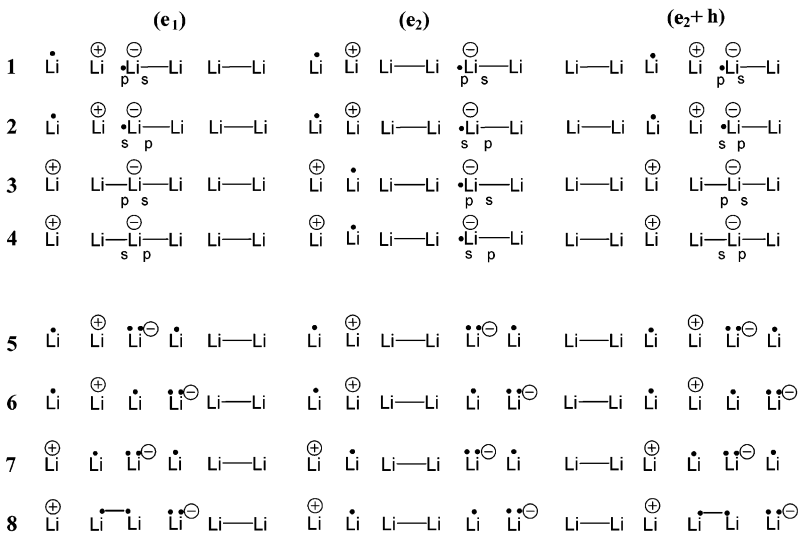

Figure 5. Canonical Lewis structures for Pauling (structures **1**−**4**) and antibonding MO (structures **5**−**8**) electron conduction mechanisms along a linear chain of six lithium atoms. For clarity, formal or "long bonds" that link singly occupied AOs on nonadjacent atoms are not included. (e_1) = first electron-transfer step, (e_2) = second electron-transfer step, and (e_2 + h) = second electron-transfer step + associated hole transfer step.

included, there is a total of 10 configurations to represent the four VB structures.

In this paper, we compare the (e_1), (e_2), and (e_2 + h) electron-transfer steps displayed in Figures 3 and 4 for the Pauling and antibonding MO mechanisms.

Method

We have used Roso's ab initio VB program[19−21] to perform STO-6G VB calculations for a linear arrangement of the lithium atoms with nearest-neighbor internuclear separations of 3.03 Å.[22a] Slater orbital exponents of 2.7, 0.65, and 0.475 were used for the 1s, 2s, and $2s^-$ AO's, respectively. (It should be noted that with atom and ion 2s AO's on the same atomic center, for the antibonding MO mechanism an equivalence exists between extended MO and VB formulations of the three-electron bond.[6,23]) For both mechanisms, the exponent of the 2p AO was determined variationally to have a value of 0.4 in the absence of an external potential. This value was used in all subsequent calculations. Of course this type of basis set is crude by current standards, but the results obtained can be used to illustrate qualitative aspects of the electron conduction process.

The $S = 0$ spin VB structures that we consider involve either two or four singly occupied AO's when Heitler−London type wave functions are used to represent covalent electron-pair bonds in these structures. For two singly occupied AO's, a and b, the Slater-determinantal wave function is $|a^\alpha b^\beta| + |b^\alpha a^\beta|$. With four singly occupied AO's, a, b, c, and d, there are two linearly independent Rumer-type wave functions, which are given by eqs 1 and 2.

$$\Psi_I = |a^\alpha b^\beta c^\alpha d^\beta| + |a^\beta b^\alpha c^\beta d^\alpha| - |a^\alpha b^\beta c^\beta d^\alpha| - |a^\beta b^\alpha c^\alpha d^\beta| \quad (1)$$

$$\Psi_{II} = |a^\alpha b^\beta c^\beta d^\alpha| + |a^\beta b^\alpha c^\alpha d^\beta| - |a^\alpha b^\alpha c^\beta d^\beta| - |a^\beta b^\beta c^\alpha d^\alpha| \quad (2)$$

For the Pauling bicovalent structure

$$Li_B - \overset{\ominus}{Li_C} - Li_D$$

the four singly occupied AO's are a = $2s_B$, b = $2p\sigma_C$, c = $2s_C$, and d = $2s_D$. In the Ψ_I, $2s_B-2p\sigma_C$ and $2s_C-2s_D$ spin-pairings occur, whereas Ψ_{II} involves $2s_B-2s_C$ and $2p\sigma_C-2s_D$ spin-pairings. When $Li^{(-)}$ 2s and 2pσ AO's are included in the antibonding MO mechanism, VB structures arise in which one-center 2pσ−2s and (nonadjacent) two-center 2s−2s spin-pairings occur. Thus for the VB structure

$$Li_B \quad \overset{\ominus}{Li_C} \quad Li_D$$

the relevant AO's are a = $2s_B$, b = $2s_C$, c = $2p\sigma_C$, and d = $2s_D$, and the appropriate $S = 0$ spin wave function is equal to $-\Psi_I - \Psi_{II}$.

When two electrons are not involved explicitly in the electron-transfer process at any stage we have, for computational simplicity, located the electrons in a doubly occupied bonding MO. For example, this MO for the Li_E-Li_F bond of the (e_1) step in Figures 2−4 is $\sigma_{EF} = 2s_E + k2s_F$, for which k is a polarity parameter whose value is determined variationally for each mechanism. For the eight atom calculations with model external potentials, we have approximated the Li_G-Li_H electron-pair bond adjacent to the anode as $Li_G^+Li_H^-$ (i.e., $k = \infty$ in $\sigma_{GH} = 2s_G + k2s_H$). Pilot calculations indicate that this approximation is satisfactory and that the values for each of the (e_1), (e_2), and (e_2 + h) polarization parameters for the six atom calculations change only slightly when the $Li_G^+Li_H^-$ is introduced.

The appropriate VB structures included in the various six atom ($Li_ALi_BLi_CLi_DLi_ELi_F$) calculations are displayed in Figure 5. (Elaboration of the calculations would use Coulson−Fischer[24] type orbitals instead of one-center AO's, thereby including additional canonical Lewis structures in the resonance schemes.) Introduction of a model external potential is achieved by locating negative (cathode) and positive (anode) charges ($Q = -1$, -2, or -3, and $Q = +1$, $+2$, or $+3$, respectively), at distances of 3.03 Å to the left of Li_A and 3.03 Å to the right of either the Li_F (six atom calculation) or the Li_H (eight atom calculation), respectively. Obviously such an approach is artificial, but it does provide insights into changes in the nature of the primary VB structures when an external potential is applied, and the energy lowering that occurs as the excited electron proceeds from cathode to anode. These choices for the magnitudes and locations of the charges are arbitrary and therefore some of our conclusions are dependent on the nature of these choices.

Weights for the VB structures have been calculated[25] using the formula $W_i = C_i^2/\Sigma C_j^2$, in which C_i is the coefficient of the normalized wave function for VB structure **i** in the ground-

TABLE 1: Li_6 and Li_8 Weights and Energies (au) for the Pauling (Structures 1−4) and Antibonding MO (Structures 5−8) Mechanisms with No External Potential ($Q = 0$)[a]

structure	(e_1) $k = 0.9$ (0.9, 1.2)	(e_2) $k = 0.1$ (1.0, 0.1)	($e_2 + h$) $k = 1.5$ (0.9, 1.5)
1	0.910, 0.910	0.899, 0.887	0.917, 0.924
2	0.017, 0.012	0.002, 0.005	0.023, 0.013
3	0.074, 0.078	0.097, 0.096	0.060, 0.062
4	0.000, 0.000	0.003, 0.012	0.000, 0.001
energy	−44.4454, −59.2657	−44.3968, −59.2183	−44.4446, −59.2654

structure	(e_1) $k = 1.0$ (0.8, 0.9)	(e_2) $k = 0.1$ (1.0, 0.1)	($e_2 + h$) $k = 1.6$ (0.9, 1.5)
5	0.811, 0.820	0.839, 0.798	0.829, 0.812
6	0.079, 0.082	0.063, 0.100	0.060, 0.085
7	0.107, 0.095	0.089, 0.086	0.105, 0.099
8	0.003, 0.002	0.009, 0.016	0.006, 0.003
energy	−44.4434, −59.2640	−44.4016, −59.2225	−44.4434, −59.2639

[a] (e_1) = first electron-transfer step, (e_2) = second electron-transfer step, and ($e_2 + h$) = second electron transfer + hole transfer step. k values in parentheses refer to $\sigma_{GH} = 2s_G + k2s_H$ and either $\sigma_{EF} = 2s_E + k2s_F$ or $\sigma_{CD} = 2s_C + k2s_D$ or $\sigma_{AB} = 2s_A + k2s_B$.

state wave function for resonance between either structures **1**−**4** or **5**−**8** of Figure 5.

Results and Discussion

In Table 1, we report Li_6 and Li_8 energies (1 au = 4.360E−18 J) and the weights for the Lewis VB structures **1**−**4** of the Pauling mechanism and **5**-**8** of the antibonding MO mechanism with no external potential. The remaining tables provide values for the Li_6 and Li_8 energies (Tables 2, 3, and 6) and Li_8 structural weights (Tables 4 and 5) with an external potential.

(a) No External Potential. The electronic structure of the conduction band will involve resonance between the Lewis-type VB structures of Figure 5, together with all other Lewis structures that will interact with them, but which do not contribute directly to the conduction mechanisms that are being considered. Here we give consideration to the nature of the primary Lewis structures for the conduction mechanisms of Figures 3 and 4.

For each of the (e_1) and ($e_2 + h$) electron-transfer processes, resonance between the Lewis structures **1**−**4** for the Pauling mechanism generates an energy which is marginally lower than that for the **5**−**8** resonance for the antibonding MO mechanism. The converse result is obtained for the (e_2) electron-transfer process. In accord with electrostatic considerations, the ($e_2 + h$) mechanisms of Figure 4, with both electron and positive hole transfer, are calculated to involve lower energies than the (e_2) mechanisms of Figure 3, with no positive hole transfer. Electrostatics also account for the large weight for either structure **1** (Pauling) or structure **5** (antibonding MO) for each of the (e_1), (e_2), and ($e_2 + h$) electron-transfer processes. The positive and negative formal charges have closer spatial locations in these structures (and also in structure **2**) than they do in the other structures. Structures **1** and **2**, with the same arrangements of formal charges, possess $2s_C-2s_D$ and $2p\sigma_C-2s_D$ bonds, respectively. However the presence of the $2s_C-2s_D$ bond in structure **1** stabilizes it relative to structure **2** with the $2p\sigma_C-2s_D$ bond.

The polarization parameter, k, for the doubly occupied bonding MO $\sigma_{EF} = 2s_E + k2s_F$ has a value near to unity for the (e_1) electron-transfer step (Figure 3). In contrast to what occurs in either of the second electron transfer steps, the absence of a positive or negative formal charge on Li_D in the dominant Lewis structures **1** and **5** ensures that the Li_E-Li_F electron-pair bond is nearly homopolar, i.e., the value of the polarity parameter k for the doubly-occupied σ_{EF} MO is near unity. Similarly, for each of the electron transfer steps, the absence of a positive or negative formal charge on Li_F in structures **1** and **5** ensures that the Li_G-Li_H electron-pair bond is almost homopolar.

In the absence of an external potential, due to symmetry, there is no preferred direction for electron transfer. The positive and negative charges ($\pm Q$) associated with the anode and cathode provide the asymmetry needed for a unidirectional flow of electrons. The results of the eight-atom calculations for $Q \neq 0$ (Tables 2−6) show that the propensity for this effect to occur increases as the magnitude of Q increases.

(b) Applied External Potential. When the external potential is applied (Tables 2 and 3), the presence of the cathode ($Q = -1$, -2, and -3) and the anode ($Q = +1$, $+2$, and $+3$) induces substantial polarization of the Li_E-Li_F and Li_A-Li_B bonds for the (e_1) and (e_2+h) electron transfers, thereby increasing the ionic character of these bonds so that they approximate to $Li_E^+Li_F^-$ and $Li_A^+Li_B^-$. However for the (e_2) electron transfer, the ionic character of the $Li_C^+Li_D^-$ bond decreases relative to that which occurs when $Q = 0$ (Table 1). The behavior of the polarization parameters is similar in the Li_6 and the Li_8 calculations.

In Tables 4 and 5, we report the weights for VB structures **1**−**8** when $Q = \pm 1$ and ± 3. They show that as the magnitude of Q increases, the importance of the (bicovalent) structure **4** for the Pauling mechanism and structure **8** for the antibonding MO mechanism increases. For large Q, these structures are calculated to be the primary Lewis structures. When $Q = \pm 1$, the other bicovalent structure **3** also makes a significant contribution to the (e_1) and the (e_2) electron-transfer processes of the Pauling mechanism.

The energies for the antibonding MO mechanism are calculated to lie marginally below the energies for the Pauling mechanism. The magnitude of the energy difference increases as the size of the external potential increases. When $Q = \pm 2$ or ± 3, this result is also obtained when the lithium $2p\sigma$ AO is excluded from the antibonding MO mechanism. Inclusion of the $2p\sigma$ AO generates only a small stabilization for the latter mechanism when $Q = \pm 3$.

(c) Energy Decrease as Electron Conduction Proceeds. The discussions of this section will be based on the results of the Li_8 calculations. For the antibonding MO mechanism, similar results are obtained for the Li_6 calculations.

As the excited electron moves from the cathode to the anode, an energy decrease must occur at each successive electron-transfer step. For both mechanisms, the total energy that arises after the second electron transfer is associated with (ground-state) (e_2) ↔ ($e_2 + h$) resonance, to give the wave function $\Psi = \Psi(e_2) + C\Psi(e_2 + h)$. When $Q = \pm 1$ (Tables 2 and 3), for both mechanisms, the energies for the (e_1) electron transfers are less than the energies for each of the (e_2) and ($e_2 + h$) electron transfers. However the (e_2) ↔ ($e_2 + h$) resonance gives Pauling and antibonding MO energies of −59.4026 and −59.4104 au (Table 6), respectively. These energies are lower than the (e_1) electron-transfer energies of −59.3950 au (Pauling) and −59.3974 au (antibonding MO).

When $Q = \pm 2$ and ± 3, the energy for the antibonding MO mechanism decreases as one proceeds from the (e_1) electron transfer to the (e_2) electron transfer (Tables 2 and 3). The energy difference $E(e_1) - E\{(e_2) \leftrightarrow (e_2 + h)\}$, as well as $E(e_1) - E(e_2)$, increases for each mechanism as the magnitude of Q increases (cf. Tables 2, 3, and 6), thereby demonstrating that an increase

TABLE 2: Energies (*E*, au) and MO Polarity Parameters (*k* in $k2s_E + 2s_F$, $2s_C + k2s_D$, or $k2s_A + 2s_B$) for the Pauling Mechanism

	6 atoms			8 atoms		
	(e_1)	(e_2)	$(e_2 + h)$	(e_1)	(e_2)	$(e_2 + h)$
$Q = \pm1$, *E*	−44.5867	−44.5686	−44.5779	−59.3950	−59.3791	−59.3916
$Q = \pm1$, *k*	0.2	0.6	0.1	0.2	0.6	0.1
$Q = \pm2$, *E*	−44.8803	−44.8501	−44.8588	−59.6714	−59.6751	−59.6557
$Q = \pm2$, *k*	−0.2	1.1	0.0	0.1	0.8	0.0
$Q = \pm3$, *E*	−45.2506	−45.2118	−45.1434	−59.9981	−60.0204	−59.9703
$Q = \pm3$, *k*	−0.3	2.5	−0.1	0.1	1.1	−0.1

TABLE 3: Energies (*E*, au) and MO Polarity Parameters (*k* in $k2s_E + 2s_F$, $2s_C + k2s_D$, or $k2s_A + 2s_B$) for the Antibonding MO Mechanism

	6 atoms			8 atoms		
	(e_1)	(e_2)	$(e_2 + h)$	(e_1)	(e_2)	$(e_2 + h)$
$Q = \pm1$, *E*	−44.5934	−44.6038	−44.5991	−59.3974	−59.3949	−59.3952
$Q = \pm1$, *k*	0.1	0.6	0.1	0.1	0.6	0.2
$Q = \pm2$, *E*	−44.9132	−44.9662	−44.9146	−59.6893	−59.7085	−59.6747
$Q = \pm2$, *k*	−0.2	1.3	−0.1	0.1	0.9	0.0
$Q = \pm3$, *E*	−45.3140	−45.4134	−45.3078	−60.0349	−60.0765	−60.0078
$Q = \pm3$, *k*	−0.3	2.7	−0.1	0.0	1.2	−0.1

TABLE 4: Li_8 Structural Weights, Energies (au), and MO Polarity Parameters (*k* in $k2s_E + 2s_F$, $2s_C + k2s_B$, and $k2s_A + 2s_B$) for the Pauling Mechanism

	$Q = \pm1$			$Q = \pm3$		
structure	(e_1)	(e_2)	$(e_2 + h)$	(e_1)	(e_2)	$(e_2 + h)$
1	0.070	0.028	0.274	0.001	0.000	0.004
2	0.012	0.022	0.047	0.001	0.006	0.003
3	0.354	0.369	0.217	0.006	0.049	0.002
4	0.564	0.581	0.463	0.991	0.945	0.991
energy	−59.3950	−59.3791	−59.3916	−59.9981	−60.0204	59.9703
k	0.2	0.6	0.1	0.1	1.1	−0.1

TABLE 5: Li_8 Structural Weights, Energies (au), and MO Polarity Parameters (*k* in $k2s_E + 2s_F$, $2s_C + k2s_D$, or $k2s_A + 2s_B$) for the Antibonding MO Mechanism[a]

	$Q = \pm1$			$Q = \pm3$		
structure	(e_1)	(e_2)	$(e_2 + h)$	(e_1)	(e_2)	$(e_2 + h)$
5	0.024	0.008	0.070	0.000	0.000	0.001
6	0.043	0.029	0.148	0.005	0.007	0.007
7	0.445	0.121	0.353	0.015	0.007	0.015
8	0.488	0.842	0.429	0.980	0.986	0.978
energy	−59.3974	−59.3949	−59.3952	−60.0349	−60.0765	−60.0078
	(−59.3853)	(−59.3880)	(−59.3823)	(−60.0329)	(−60.0750)	−60.0060
k	0.1	0.6	0.2	0.0	1.2	−0.1
	(0.1)	(0.6)	(0.2)	(0.0)	(1.2)	(−0.1)

[a] Energies and polarity parameters in parentheses omit the 2p AOs.

TABLE 6: Li_8 Energies (au) for the $(e_2) \leftrightarrow (e_2 + h)$ Resonance, with (e_2) and $(e_2 + h)$ *k* Values of Tables 2 and 3

	$Q = \pm1$	$Q = \pm2$	$Q = \pm3$
Pauling	−59.4026	−59.6840	−60.0255
antibonding MO	−59.4104	−59.7140	−60.0796

in the magnitude of the external potential increases the tendency for electron transfer to occur between the cathode and anode.

Of course, for each value of $|Q|$, the $(e_1) \leftrightarrow (e_2) \leftrightarrow (e_2 + h)$ resonance occurs, with the restricted wave function $\Psi = C_1\Psi(e_1) + C_2\Psi(e_2) + C_3\Psi(e_2 + h)$ associated with it. To provide a simple example of this wave function, we have constructed it for the antibonding MO mechanism, when $Q = \pm3$. For these values of *Q*, the weights reported in Table 5 show that structure **8** is the dominant type of Lewis structure for each of the electron-transfer steps. With the $2p\sigma$ AO omitted from the calculations, the energies for $\Psi(e_1)$, $\Psi(e_2)$ and $\Psi(e_2+h)$, −60.0318, −60.0725, and −60.0049 au are similar to those obtained when structures of types **5**−**7** are also included in the calculations (−60.0329, −60.0750, and −60.0060 au; cf. Table 5). For the $(e_1) \leftrightarrow (e_2) \leftrightarrow (e_2 + h)$ resonance, we obtain $\Psi = 0.31884\Psi(e_1) - 0.75041\Psi(e_2) + 0.14218\Psi(e_2 + h)$, with an energy of −60.0820 au. The resulting weights for the (e_1), (e_2), and $(e_2 + h)$ structures of type **8** are 0.223, 0.702, and 0.076, thereby showing the dominance of the $(e_2) \leftrightarrow (e_2 + h)$ resonance over the (e_1) step.

For $Q = \pm3$ (with the $2p\sigma$ AO omitted), the energies for the type **8** (e_1), (e_2), and $(e_2 + h)$ structures, −60.0318, −60.0725, and −60.0049 au, are lower than the corresponding (e_1), (e_2), and $(e_2 + h)$ energies of −59.9981, −60.0204, and −59.9703 au (Table 4) for the Pauling mechanism. For the latter mechanism, the structural weights of Table 4 indicate that structure **4** is the dominant type of structure. For each of the structures of type **8**, the negative charge is located closer to the anode and further from the cathode than it is in the corresponding structure of type **4**. Therefore for large *Q*, electrostatic considerations are in accord with the calculated result that the antibonding MO mechanism involves a lower energy.

To separate the (e_1) from the $(e_2) \leftrightarrow (e_2 + h)$ electron-transfer step, we require $\langle\Psi(e_1)|\Psi\rangle = \langle\Psi(e_1)|H|\Psi\rangle = 0$, with $\Psi =$

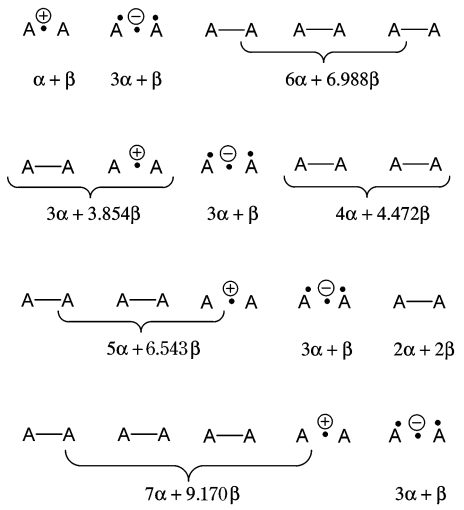

Figure 6. VB structures for each electron transfer step together with the Hückel energies for the positively charged and neutral "polyene" separated by the three-electron bond that carries the negative charge.

$C_1\Psi(e_1) + C_2\Psi(e_2) + C_3\Psi(e_2 + h)$. The resulting wave function for the type **8** Lewis structures is $\Psi = -0.03583\Psi(e_1) + \Psi(e_2) + 0.88520\Psi(e_2 + h)$, whose energy, -60.0352 au, lies slightly below the energy of -60.0318 au for the $\Psi(e_1)$ energy.

The $(e_2) \leftrightarrow (e_2 + h)$ resonance for the second electron transfer can be generalized. For the *n*th electron transfer, there are *n* positive holes, h_1, h_2, ..., h_n. The resulting wave function associated with the $(e_n + h_1) \leftrightarrow (e_n + h_2)... \leftrightarrow (e_n + h_n)$ resonance is $\Psi_n = C_1\Psi(e_n + h_1) + C_2\Psi(e_n + h_2) + ... + C_n\Psi(e_n + h_n)$. This wave function should approximate to either $\Psi_n = C_{n-1}\Psi(e_n + h_{n-1}) + C_n\Psi(e_n + h_n)$ for small Q or $\Psi_n = C_1\Psi(e_n + h_1) + C_2\Psi(e_n + h_2)$ for large Q.

Further energy lowerings are obtained by interacting the VB configurations for the Pauling structures **1**−**4** and the antibonding MO structures **5**−**8**, but for the present purpose, it is not necessary to do this.

(d) Hückel MO Theory and Electron Transfer. The energy lowering of the second step relative to the first step is associated in part with the greater degree of delocalization of the positive charge in the second step—particularly when the external potential has a small magnitude. This is equivalent to the existence of a larger resonance stabilization energy for the associated electrons in the resulting $(Li_ALi_BLi_CLi_D)^+$ cation, compared with what occurs in the $(Li_ALi_B)^+(Li_ELi_F)$ for the first step. The effect can be illustrated simply by using Hückel MO theory for a linear polyene with equally spaced atoms, when no external potential is applied.

The Hückel MO energies are given[22b] by $e_i = \alpha + 2\beta\cos(i\pi/(N + 1))$, in which α and β are the Coulomb and (negative) nearest-neighbor resonance integrals, N is the number of atoms in the polyene, and $i = 1$ to N. The total Hückel MO energy is $E = \Sigma\nu_i e_i$, in which ν_i is the occupation number for the ith MO with energy e_i. We provide one example here for a chain of 10 atoms using the VB symbolism for the antibonding MO mechanism, with three electron transfers after the initial step. The VB structures for each electron transfer step are displayed in Figure 6, together with the Hückel energies for the positively charged and neutral "polyene", which are separated by the three-electron bond that carries the negative charge. Each three-electron bond has a Hückel energy of $3\alpha + \beta$. The (negative) resonance energies of 8.988β, 9.326β, 9.543β, and 10.170β increase in magnitude as the conduction electron proceeds along the chain of atoms.

A similar result is obtained from the free electron model for electrons in a 1-dimensional box. The energy levels are given by $e_n \propto n^2/L^2$, with $n = 1, 2, 3, ...$ and $L =$ box length. The box length is given by $L = (N - 1)R$, in which N is the number of equally spaced atoms and R is the spacing between a pair of adjacent atoms. With $E \propto \Sigma\nu_i e_i$, the energies for each electron-transfer step of Figure 6 are proportional to the following values: $(6 + 53/25)/R^2$, $(6 + 16/9)/R^2$, $(6 + 69/25)/R^2$, and $(6 + 44/49)/R^2$. They show that the lowest energy is obtained for the $A_8^+A_2^-$ system (i.e., $(6 + 44/49)/R^2$), which involves the greatest degree of delocalization of positive charge.

Conclusions

When an external electric potential is applied across a linear chain of eight lithium atoms, the results of model VB calculations indicate that (a) the electronic structure of the conduction band changes substantially, with the development of essentially ionic character at the diatomic Li−Li sites adjacent to the cathode and the anode in particular, (b) the propensity for electron transfer to occur between cathode and anode increases as the size of the potential increases; (c) the energy at each stage of the electron transfer process is lower for the antibonding MO mechanism than it is for the Pauling mechanism, and finally, (d) for small external potentials, electron transfer from the first step to the second step is assisted by a greater extent of delocalization of positive charge. Conclusion (d) is equivalent to saying that the associated electrons for a positively charged "polyene" are more delocalized after the second electron-transfer step than they are after the first step, thereby leading to a "crucial reduction" in the kinetic energies of these electrons.[26]

With or without an external potential, electrostatics primarily determine which Lewis-type VB structures are important at each stage of the electron-transfer process.

We stress that the above conclusion (c) in particular is based on the nature of the external potential and the number of lithium atoms that we have considered, and therefore, this conclusion is obviously model-dependent.

Increased-valence structure representations based on those used for gas-phase nucleophilic substitution reactions[6,27] can be developed for electron conduction.

Acknowledgment. We are grateful to and thank the following people: (a) Dr. W. Roso for his ab initio VB program and Dr. F. L. Skrezenek for installing it; (b) the Victorian Partnership for Advanced Computing, grant number EPPNNU0024/2001; (c) Dr. J. M. White for support; and (d) Dr. H. M. Quiney for reading the manuscript. During the later stages of the project, Dr. White also provided an improved workstation. Dr. Quiney then installed the VB programs on the workstation and ensured that the time needed to perform the calculations could be decreased dramatically.

References and Notes

(1) Pauling, L. *Nature* **1948**, *61*, 1019.
(2) Pauling, L. *Proc. R. Soc.* (London) **1949**, *A196*, 343.
(3) Pauling, L. *J. Solid State Chem.* **1984**, *54*, 297.
(4) Pauling, L.; Herman, Z. S. In *Valence Bond Theory and Chemical Structure*; Klein, D. J., Trinajstić, N., Eds.; Elsevier: Amsterdam, 1990; p 569 (see also refs 4 and 6 therein).
(5) Herman, Z. S. In *Pauling's Legacy Modern Modelling of the Chemical Bond*; Maksić, Z. B., Orville-Thomas, W. J., Eds.; Elsevier Science: Amsterdam, 1999; p 701 (see also refs 25 and 27 therein).
(6) Harcourt, R. D. In *Pauling's Legacy Modern Modeling of the Chemical Bond.*; Maksić, Z. B., Orville-Thomas, W. J., Eds.; Elsevier Science: Amsterdam, 1999; p 449.

(7) Harcourt, R. D. *Qualitative Valence-Bond Descriptions of Electron-Rich Molecules: Pauling "3-Electron Bonds" and "Increased-Valence" Theory*; Lecture Notes in Chemistry; Springer-Verlag: Berlin, Heidelberg, New York, 1982; Vol. 30, p 230.

(8) Harcourt, R. D. *J. Phys. B* **1974**, *7*, L41.

(9) Pavão, A. C.; Taft, C. A.; Guimarães, T. C. F.; Leão, M. B. C.; Mohallem, J. R.; Lester, W. A. *J. Phys. Chem. A* **2001**, *105*, 5.

(10) Harcourt, R. D. In *Valence Bond Theory*; Cooper, D., Ed.; Elsevier Science: Amsterdam, 2002; p 349. In this reference, consideration is given to entrance into the conduction band via the Pauling and antibonding MO mechanisms. Four atomic centers are involved with no external potential. The energies cited exclude nuclear repulsion.

(11) McAdon, M. H.; Goddard, W. A. *J. Phys. Chem.* **1987**, *91*, 2607.

(12) Tornaghi, E.; Cooper, D. L.; Gerratt, J.; Raimondi, M.; Sironi, M. *Croat. Chem. Acta* **1991**, *64*, 429.

(13) Tornaghi, E.; Cooper, D. L.; Gerratt, J.; Raimondi, M.; Sironi, M. *J. Mol. Struct. THEOCHEM* **1992**, *91*, 383. Raimondi, M.; Tornaghi, E.; Cooper, D. L.; Gerratt, J. *J. Chem. Soc., Faraday Trans.* **1992**, *88*, 2309.

(14) Mohallem, J. R.; Vianna, R. O.; Quintão, A. D.; Pavão, A. C.; McWeeny, R. *Z. Phys. D—At. Mol. Clusters* **1997**, *42*, 135.

(15) Quintão, A. D.; Vianna, R. O.; Mohallem, J. R. *Eur. Phys. J. D* **1999**, *6*, 89.

(16) Quintão, A. D.; Vianna, R. O. *Int. J. Quantum Chem.* **2001**, *81*, 76.

(17) Vianna, R. O.; Quintão, A. D. In *Valence Bond Theory*; Cooper, D., Ed.; Elsevier Science: Amsterdam, 2002; p 379.

(18) de Visser, S. P.; Danovich, D.; Wu, W.; Shaik, S. *J. Phys. Chem. A* **2002**, *106*, 4961 and ref 10 therein.

(19) Harcourt, R. D.; Roso, W. *Can. J. Chem.* **1978**, *56*, 1093.

(20) Skrezenek, F. L.; Harcourt, R. D. *J. Am. Chem. Soc.* **1984**, *106*, 3934.

(21) Harcourt, R. D.; Pyper, N. *Int. J. Quantum Chem.* **1998**, *68*, 129.

(22) McWeeny, R. *Coulson's Valence*, 3rd ed.; Oxford University Press: Oxford, U.K., 1979; (a) p 326, (b) p 241.

(23) Harcourt, R. D. *J. Phys. Chem. A* **1997**, *101*, 2496, 5962.

(24) Coulson, C. A.; Fischer, I. *Philos. Mag.* **1949**, *40*, 386.

(25) Bachler, V. *Theor. Chem. Acc.* **1997**, *92*, 223 and refs 55 and 56 therein.

(26) Ruedenberg, K. *Rev. Mod. Phys.* **1962**, *34*, 326.

(27) Harcourt, R. D. *J. Mol. Struct. (THEOCHEM)* **1997**, *398*−*399*, 93 and refs 15 and 16 therein.